Journal of King Saud University – Science 34 (2022) 101689

Contents lists available at ScienceDirect

Journal of King Saud University – Science

journal homepage: www.sciencedirect.com

Original article

Investigations on amidoxime grafted sepiolite based chitosan organic–inorganic nanohybrid composite beads towards wastewater detoxification

Mohib Ullah Khan [a], Bandar Ali Al-Asbahi [b,*], Saira Bibi [a], Shaista Taimur [c], Mohsan Nawaz [a], Tariq Yasin [c], W. Aslam Farooq [b,*], Zarshad Ali [a], Iram Bibi [a], Saddiqa Begum [a], Ali Bahader [a], Zia ur Rehman [d], Nafeesah Yaqub [b], Abdullah Ahmed Ali Ahmed [e]

[a] Department of Chemistry, Hazara University, Mansehra 21300, Pakistan
[b] Department of Physics & Astronomy, College of Science, King Saud University, P.O. Box 2455, Riyadh 11451, Saudi Arabia
[c] Department of Chemistry, Pakistan Institute of Engineering and Applied Sciences, Islamabad 45650, Pakistan
[d] Department of Mathematics, Namal Institute, Mianwali, Pakistan
[e] Center for Hybrid Nanostructures (CHyN) and Fachbereich Physik, Universität Hamburg, 20146 Hamburg, Germany

ARTICLE INFO

Article history:
Received 24 June 2021
Revised 29 October 2021
Accepted 1 November 2021
Available online 3 November 2021

Keywords:
Nanohybrid
Sepiolite
Composite
Chitosan
Copper
Methylene blue

ABSTRACT

This work explores the fabrication of organic–inorganic nanohybrid based biopolymer composite systems for the cleaning of different contaminants from wastewater. This system involves the simultaneous radiation grafting techniques for sepiolite (SP) modification and the simple mixing of modified-SP with biopolymer matrix, chitosan (CS). The SP beads were chemically modified with amidoxime prior to its use in composite systems. The synthesized composite beads were characterized using scanning electron microscopy (SEM), thermal gravimetric analysis (TGA), nitrogen physical adsorption (BET) investigations, Fourier transform infrared (FT-IR), atomic absorption and UV–visible spectroscopy. Hydrolytic stability of beads was also investigated in aqueous media, beads showed excellent stability in aqueous medium and in acidic environment. Here, the sorption profile of copper over amidoxime grafted SP-nanohybrid (MSP) incorporating CS-beads is reported. Furthermore, the key adsorptive variables, i.e. contact time, adsorbent dose, and concentration of adsorbate are discussed. Different isothermal (Langmuir and Freundlich) and kinetics model were also elaborated. Langmuir isotherm and pseudo-second-order models are proved to be the best fit models for Cu (II) removal in aqueous system. To explore the efficacy of the material towards organic pollutants, methylene blue (MB) was selected as model compound and adsorbed on nanohybrid beads. The results revealed that organic–inorganic nanohybrid incorporating CS beads are quite effective for contaminated water remediation, owing to their better adsorptive performance, high stability and easy application.

1. Introduction

Water is crucial to the existence of living organisms in the environments. Unfortunately, clean water resources are affected by the wide increase in industrialization and modernizations (Ay et al., 2012; Salama et al., 2015). Living organisms are endangered by water contamination produced by release of numerous organic and inorganic harmful compounds into water resources (Arun et al., 2020). Organic dyes and heavy metals, are the leading contaminants in effluent imparting extremely harmful influence on human health and environment (Aldalbahi et al. 2020; Nawaz et al., 2020; Zhang et al., 2020). Depending on the concentrations of toxic metals such as lead, chromium, cadmium, mercury, and

* Corresponding authors.
E-mail addresses: balasbahi@ksu.edu.sa (B.A. Al-Asbahi), awazirzada@ksu.edu.sa (W.A. Farooq).

Peer review under responsibility of King Saud University.

Production and hosting by Elsevier

https://doi.org/10.1016/j.jksus.2021.101689
1018-3647/

copper in water altogether threaten the ecosystems. Presence of water pollutants even in very low concentrations are reported to cause mutagenic effects, thus leading to serious health threats such as cancer etc. (Vidu et al., 2020). Presence of dyes in water can reduce the photosynthetic activity as well (Bharti et al., 2021).

In the last few decades, hybrid materials having both organic and inorganic moieties have received a great focus of the environmental scientists and engineers (Azeez et al., 2013). Such hybrid materials can be used for the removal of various kinds of toxic pollutants from wastewater. Among such hybrid materials, polymer/clay-based systems are recognized as best regarding their exceptional adsorptive characteristics. Owing to the occurrence of tunable functional groups, high surface area, the clay has been used successfully for removing many organic pollutants (Parisi, 2020), metal ions and dyes from wastewater (Mansoori et al., 2010). Amongst the clays, sepiolite holds superior position because of its morphological importance. Silanol groups (Si-OH) are concentrated at the outer surface of the fibers (sepiolite) due to periodic transposition of the silica sheets (Ruiz-Hitzky et al., 2013). These groups could be utilized to incorporate various organic moieties which may include polymers and coupling agents (Galan, 1996; García et al., 2011). It has been found that amidoxime grafted groups on sepiolite have a strong affinity to form chelate complex with metal ions (Xie et al., 2015; Ji et al., 2017). One of the most attractive procedure for the incorporation of surface groups is "grafting". It is the technique which can be used to alter the surface characteristics of material as per demand (Bhattacharya and Misra, 2004). By mean of this method, the grafting of a monomer on sepiolite is a rare idea. Previously, our group successfully synthesized new nanohybrid material by simultaneous radiation grafting method (Nasef and Güven, 2012; Badawy and Dessouki, 2003). The acrylonitrile grafted nanohybrids were chemically modified with amidoxime chelating adsorbent (Taimur et al., 2017). To explore it further, and to check the efficiency of nanohybrid towards organic–inorganic pollutants removal and for easy processing this material can be combined with polymers.

Nowadays, the scientists are focusing on the use of bio-polymer as adsorbents (Malerba and Cerana, 2020). Amongst them, chitosan is considered as one of the best choices due to its cationic nature (Li and Huang, 2013). The presences of –OH and $–NH_2$ functional groups on chitosan have great potential for the adsorption of toxic substances (Doğan et al., 2008). Furthermore, this material is very flexible and can be easily converted into desired form i.e. films/membranes or beads etc. (Bibi et al., 2016; Bibi et al., 2015). The use of chitosan as supporting material for sepiolite nanohybrid could be a good idea. In practical applications the adsorbents separation is a very important. Conventional separations such as sedimentation and filtration generally lead to the loss of adsorbents, which results in environmental problems because of the leaching of adsorbents and adsorbate. Recently, our group developed amidoxime grafted sepiolite based chitosan nanohybrids and explored their adsorptive performance for the removal of organic–inorganic pollutants. Kamal and co-workers (Kamal et al., 2016) prepared chitosan beads by crosslinking and used them for copper removal, despite the good performance, these beads were not effective in acidic environments.

In current work, we aimed to combine amidoxime grafted sepiolite with chitosan and to develop a new biopolymer based organic–inorganic-hybrid system. As stated above our group already have synthesized nanohybrid powder by grafting amidoxime groups on sepiolite surface (Alhaddad et al., 2012), and now efforts are made to develop sepiolite beads using chitosan as supporting material which are expected to perform better in neutral, acidic and basic media.

2. Materials and methods

2.1. Chemicals and materials

Acrylonitrile (99%), acetic acid (99%), acetone (99%), chitosan (degree of acetylation 75%, C-3446), methylene blue (95%) (MB) ($C_{16}H_{18}ClN_3S$), sodium hydroxide (NaOH 97%), hydrochloric acid (HCl 37%), ethanol (96%), methanol (99%), sepiolite (SP), *iso*-propanol (70%), vinyl tri-ethoxy silane (VTES 97%), dimethylformamide (DMF 98%), hydroxylamine hydrochloride (98%), sodium carbonate (99%), copper sulphate (98%) ($CuSO_4{\cdot}5H_2O$) all were obtained from Sigma Aldrich and used without further purification. Distilled water was used in all experiments.

2.2. Modification of sepiolite and beads synthesis

2.2.1. Sepiolite modification

Sepiolite (SP) was salinized as previously reported by our group (Taimur and Yasin, 2017). 10 g of SP were dispersed mechanically in distilled water (1 L, 24 h) then filtered, dried and crushed into fine powder. The crushed powder was dispersed in *iso*-propanol in a beaker while adding VTES (hydrolyzed) drop wise and stirred (2 h at 60 °C). This suspension was filtered, washed with ethanol and dried in vacuum. *Simultaneous radiation grafting (SRG):* The acrylonitrile monomer and modified SP were added to a flask. Before the addition of these reagents, the flask was exiled and purged with nitrogen. The mixture was then thoroughly stirred (8 h) in inert conditions, allowing to produce an even suspension, which was then treated by gamma rays at 5.0 (KGy) with the rate of 5.84 (kGy/h) at room temperature at NIFA (Nuclear Institute of Food and Agriculture Peshawar, Pakistan). After irradiation, the sample (RGS 5) was pulverized (FRITSCH pulverisette 6) for 1 h at 200 rpm. The sample was washed with acetone and Soxhlet extracted for 8 h with the solvent dimethylformamide to eliminate homopolymer and unreacted monomer. The sample was vacuum dried until constant weight is achieved. *Amixdoximation of SP (modified):* In this process conversion of nitrile (–C≡N) to amidoxime (AO, $–C(NH_2)$-NOH is achieved on radiation grafted sepiolite. Previously modified clay (as above) was dipped in 10 g of hydroxylamine hydrochloride solution dissolved in methanol–water (v/v = 1:1) system that contained 7.5 g of sodium carbonate. The solution pH was maintained in the range of 7.0 ± 0.5 and slowly refluxed at a temperature of 80 °C and stirred for 6 h. In order to eliminate unwanted constituents, the sample was washed with deionized water and vacuum dried at 60 °C and labelled as MSP.

2.2.2. CS/modified sepiolite composite beads fabrication

CS (3.6 g) was liquefied in 2% acetic acid solution (100 mL) in glass vial. MSP (0.292 g) was mixed to CS solution while stirring at 25 °C to achieve homogeneous blend. Then the CS-Clay blend was sonicated for 7 h at room temperature to achieve homogeneity. Gelling bath (NaOH, 10%, w/v solution) was prepared for beads fabrication. Chitosan/Clay dispersion was taken in disposable syringe (5 mL/cc), added drop wise to gelling bath and continuously stirred to form sphere beads. Beads were stirred in gelling bath for 1 h and then washed several times until neutral pH. Blank beads (CS-0) were also synthesized by using same method.

2.3. Characterization and measurements

SEM (JEOL SEM-6480LV, 120 kv) was used to examine the composite exterior morphology. The composite beads were immersed in water and freeze dried before SEM analysis. The infrared spectra were recorded on FTIR spectrophotometer (Nicolet 6700, Thermo

Electron Corp, and Waltham, Massachusetts, USA) at scanning range of 3500–500 cm^{-1}. 116 scans (average) were testified at resolution of 6.0 cm^{-1}. To study the thermal analysis of beads, Mettler–Toledo thermal gravimetric analyzer (analytical/SDTA851) was used. For TGA the temperature ranges from 50 to 700 °C (rate, 20 °C/min). To determine the surface parameters of CS-0 and CS-MSP, Brunauer–Emmett–Teller (BET) experiments were performed by surface area and porosity analyzer (Auto-sorb-IC, Quanta chrome). The hydrolytic stability of sepiolite-based chitosan beads was checked by immersing beads in water. A definite amount of composite bead was dipped in acidic, basic and neutral solutions. The stability of the beads was determined at different time intervals (up to a year).

2.4. Applications

The newly synthesized composite beads were used for the uptake of toxic metal and dye from water. On the way to evaluate the effectiveness of the material as adsorbent, copper and MB were selected as model compounds.

2.4.1. Batch adsorption studies

1000 ppm (1.575×10^{-2} M) stock solution of $CuSO_4{\cdot}5H_2O$ was prepared. Required strengths of solution (30–190 mg/L) was achieved by further dilution of this stock solution. Taking 50 mL in two reagent bottles from 30 mg/L (4.724×10^{-4} M) diluted solution and then known amount of CS-0 and CS-MSP beads were added. The bottles were kept on shaker for 3 h. After 3 h shaking, the solvent color was gradually vanished which was supposed to be adsorbed on the composite beads. To confirm adsorption, the sample was analyzed by the atomic absorption spectrophotometer (SpectrAA.300 plus, Varianuble beam). A same procedure was repeated for 50–210 mg/L range to study the effect of concentration of adsorbate for isothermal adsorption measurements. For kinetic study, 30 mg L^{-1} solution was prepared from the same standard solution. Adsorption experiments were carried out at room temperature by varying contact time (5–210 min). The remaining amount of copper ions in solution were detected by using atomic absorption spectrophotometer and calculated by using reported formula (Kamal et al., 2017).

The beads were also examined for the adsorption study of MB. The MB was dissolved to prepare 50 mgL^{-1} solution (stock) and was further diluted to 5 mg/L. The solution was taken in two reagent bottles and known amount of CS-0 and CS-MSP beads were added. Adsorption experiment at room temperature was conducted by varying contact time (5–30 min) and analyzed with UV–Visible spectrophotometer.

3. Results and discussions

3.1. Characterization of composite beads

The surface morphology of synthesized composite was studied by means of SEM. The micrographs of blank beads at various magnifications are shown in Fig. 1a. The images illustrated the porous nature of the material. Fig. 1b demonstrates SEM micrograph of CS-MSP beads. The images showed that after the addition of filler the porosity of polymer is greatly changed. However, the consistent dispersion of nanohybrid into polymer (MAG 1000 kx, 2500 kx and 5000 kx) was also detected. In addition, the micrographs also represent that no phase separation occurred which is a sign of good dispersion of filler. The main reason for the well dispersion of filler is the existence of functional groups (hydroxyl, amino and silane groups) on surface of modified clay making them more compatible with the polymer. The role of ultrasonic radiation also helps in better dispersion.

The FTIR spectra of blank chitosan and sepiolite-based chitosan synthesized beads are depicted in Fig. 2a which represent N–H (corresponds to amino group) and O–H (corresponds to hydroxyl group) stretching vibrations in the range of 3100–3500 cm^{-1}. C–H stretching can be observed around 2926 cm^{-1}. Kamal's group (Kamal et al., 2017) reported the smiler bands corresponding to the characteristic groups of functional groups present in chitosan structure. Similarly Cuevas-Acuña and co-authors (Cuevas-Acuña et al., 2021) conveyed the chitosan bands on or after 3405–900 cm^{-1} which typically links to the stretching vibrations of bonds of the amino group (NH), the stretching of the O–H links. And of course, the protonation of the amino groups of the polymer further down low pH (acidic conditions). Furthermore, the stretching vibrations of the C–O primary alcohol group (–CH_2OH), and sucrose glycoside connection (C–O–C) were also presented as also appeared.

Peak appeared at 1653 cm^{-1} corresponds to C=O stretch (due to amide group). Subsequently by the addition of nanohybrid filler, the intensity of all characteristic peaks decreased to some extent which represents the interactions of nanohybrid with polymer matrix. Both the amino and hydroxyl groups present on chitosan structure can interact with nanohybrid functional groups as shown in Fig. 4c. The spectra of both composites after copper ions uptake are shown in Fig. 2b. After copper ions uptake the characteristic peaks of both functional groups present on chitosan are somewhat shifted to the lower wavenumber which represents the interaction of metal ions with beads. This effect is more pronounced in case of nanohybrid beads. In view of the recorded spectrum for copper ion loaded nanohybrid filled beads it can be observed that all type of functional groups may involve in complexation process (H–O, Cu, N–H). The peak corresponds to N–O stretch around 915 cm^{-1} is also shifted and becomes weaker which indicates the chelation of copper ions with amidoxime group as reported earlier by our group (Taimur et al., 2017). In addition, the peak around 1019 cm^{-1} is more widen which attributes to O–Cu–O vibration (yellow circled, 2b). Fig. 2c represents the MB loaded spectra of composite beads. In this case, it can be observed that the peak intensities of characteristic bands are also slightly shifted, reflecting the interactions of MB with beads. Photographs of composite beads earlier and after copper ions uptake are presented in Fig. 2d and e, respectively.

Thermal analysis of composite beads is represented in Fig. 3. Single step degradation could be detected in both cases. Degradation started at 294.69 °C with 20.10% weight loss, owing to the moisture loss, more prominently due to elimination of the bound water (Islam et al., 2016). The thermal degradation response is quite similar from initial to around 300 °C and the thermal degradation of clay-based beads is decreased as compared to blank beads. The increased stability of CS-MSP beads can be seen until the high temperature. In case of CS-MSP the % residue is higher in comparison to CS-0 (Table 1). It can be assumed that the addition of clay may enhance the thermal stability of CS resulting in good dispersion of filler due to interactions among functional groups incorporated after clay modifications.

BET results of the nitrogen adsorption/desorption are shown in Table 1. The surface area and pore volume of chitosan is decreased after the addition of nanohybrid material. However, the pore size slightly increased in case of CS-MSP beads. The lowering of surface area might be due to the effect of grafting on nanohybrid (Taimur and Yasin, 2017). These results are consistent with SEM analysis. If we compare the SEM micrographs with same magnification, there is a systematic change from a spherical shape to a partial planar structure, and this might probably reduce the effective surface area. The hydrolytic stability of synthesized composite beads were

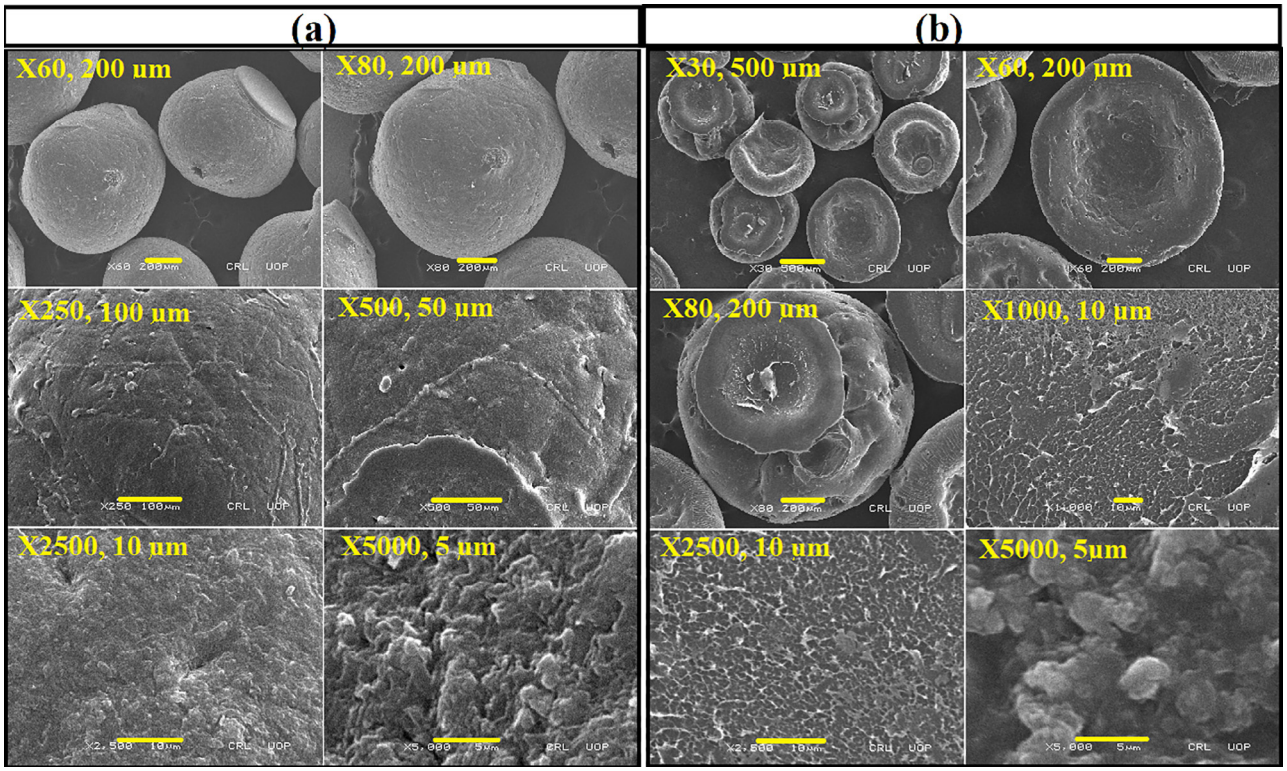

Fig. 1. SEM micrograph of composite beads: CS-0 (a) and CS-MSP (b).

observed in acidic, basic and neutral media. Known amount of synthsized beads were suspended in aqoues medium (basic, acidic and neutral) and noted the stability time. It is already reported (Wu et al., 2009) that chitosan beads are unstable in acidic enviornment because of their swelling properties. The functional groups like hydroxyl, carbonyl and amine that have not participated in cross linking are available for reaction with water and lead to polymer chain decomposition. The addition of modified SP as a filler in CS matrix, can improve the hydrolytic stability of the CS beads and make them highly stable in acidic media. This effect might be due to the crosslinking of silane groups on the surface of clay. Due to the stability in acidic medium, this type of beads can be used for the removal of toxic pollutants present in acidic environment. The beads also showed excellent stability in aqueous medium (neutral pH). In basic medium the beads are stable for several months and may last for few years. The hydrolytic stability of the CS-MSP shows better result in acidic medium as compared to CS-0 (Table 1).

3.2. Batch mode adsorption studies

3.2.1. Effect of contact time on Cu (II) uptake

The effect of time for copper ions uptake on composite beads were studied at different time intervals, 0–250 min and the results are shown in Fig. 4. It can be observed from Fig. 4a that during 15 min, the blank beads (CS-0) adsorbed 22 mg/g whereas the clay-based beads adsorbed up to 70 mg/g. The adsorption performance of both types of beads slowly increased with increasing interaction time and eventually equilibrium was established. In case of CS-0 equilibrium was reached after 3.5 h while for CS-MSP it reached after 3 h. The adsorption effect is noticeable in case of CS-MSP, as adsorption capacity was enhanced to 99 mg/g after 24 h. It can be concluded that the adsorption efficiency of chitosan can be enhanced by the addition of nanohybrid material. This enhanced capacity might be due to the occurrence of more functionalities on the surface of filler which can couple with metal ions through complexation. The proposed mechanism of the process is shown in Fig. 4c.

3.2.2. Effect of adsorbent dose

The adsorption of CS-0 beads and CS-MSP were studied at various concentrations of Cu ions solution. For this purpose, the solutions of various concentrations were prepared ranging from 30 to 190 mg/L and the adsorption capacities of synthesized beads (CS-0 and CS-MSP) were calculated. After 60 mg/L chitosan beads adsorbed 47 mg/g metal ions while at 130 mg/L and 170 mg/L adsorbed 71 mg/g and 76 mg/g, respectively. The adsorption capacity of the CS-MSP beads were gradually increased by increasing the concentration which indicates the presence of active sites on the adsorbent. The Fig. 4b, shows that the adsorption capacity was levelled off at 170 mg/L, CS-MSP beads had shown highest adsorption capacity of 92 mg/g at 190 mg/L as compared to CS-0 beads.

3.3. Adsorption kinetics

Adsorption kinetic behavior explains the adsorbent-adsorbate relationship with time. To elucidate the mode of adsorption, two kinetic models were applied to sorption data, the pseudo-first and pseudo-second-order.

3.3.1. Pseudo-first-order kinetic model

This model explains that, the extent of adsorption is directly proportional to the number of active sites present on the adsorbent surface. The linear expression for first order is represented as (Yuh-Shan, 2004):

$$ln(Q_e - Q_t) = lnQ_e - K_1 t \quad (1)$$

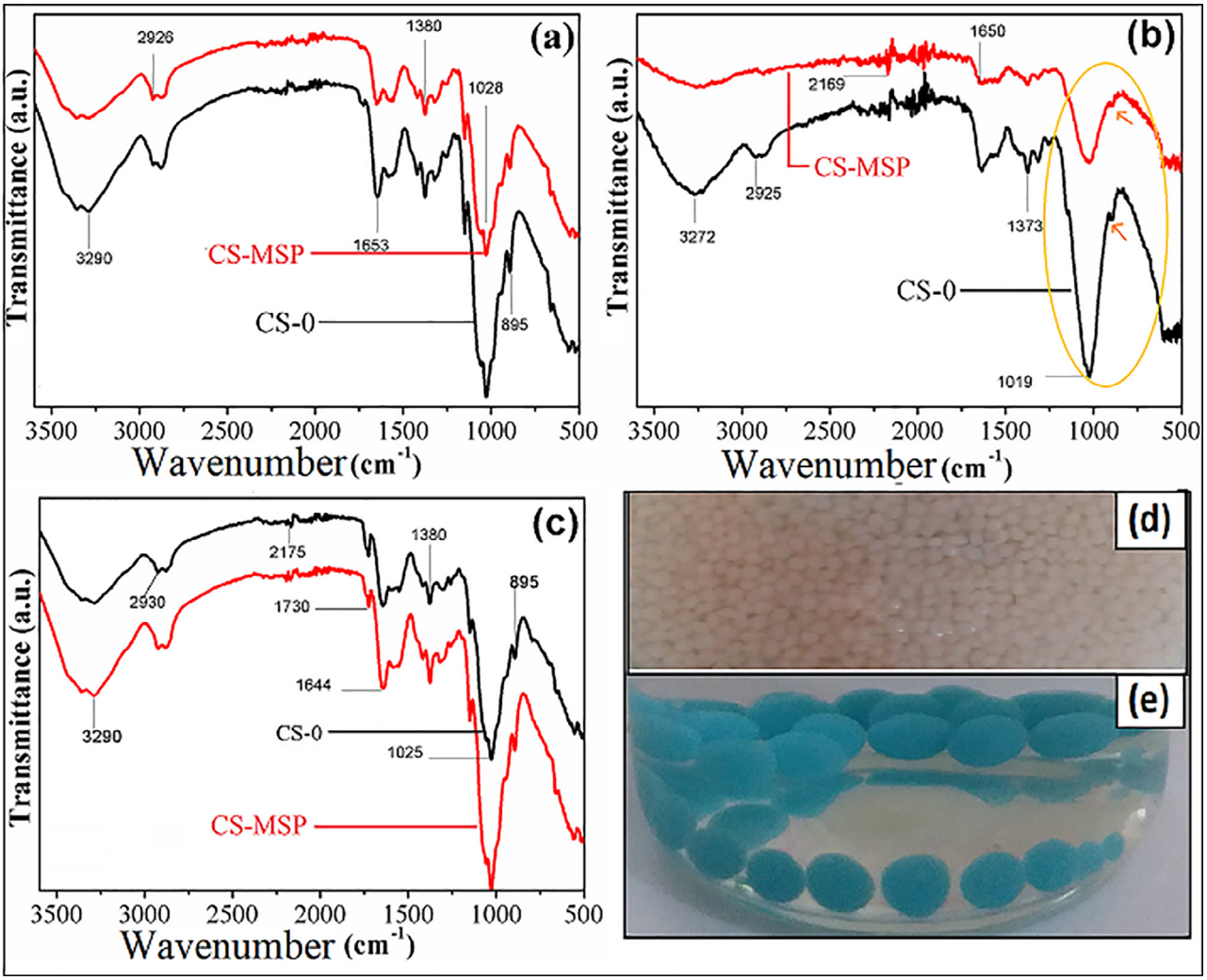

Fig. 2. FTIR spectra of composite beads (a) before Cu (II) adsorption, (b) after copper loading, (c) MB loaded CS-0, CS-MSP beads, photographic images of beads before (d) and after (e) Cu (II) uptake.

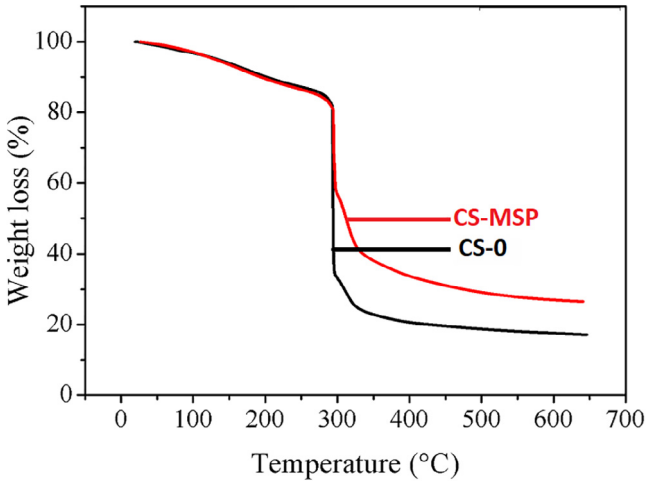

Fig. 3. Thermogram of CS-0 and CS-MSP composite beads.

Q_e and Q_t are the amount of metal that is adsorbed (in mg/g) at equilibrium and time t, respectively. K_1 is the rate constant of pseudo-first order.

3.3.2. Pseudo-second-order model

According to pseudo-second-order kinetics model, the adsorption rate is proportional to square of the amount of vacant adsorption sites. The mathematical form of the model is given as (Ho, 2006):

$$\frac{t}{Q_t} = \frac{1}{K_2 Q_e^2} + \frac{t}{Q_e} \quad (2)$$

where K_2 is the rate constant (g/mg min^{-1}) for second order.

The contact time effect on two adsorbents for metal ions uptake is shown in Fig. 5. Initially, during 20 min of interaction the adsorption of Cu ions was very abrupt, and it became maximum after 3 h and onwards it became smooth Fig. 5a. The graph based on experimental data is plotted for log (Q_e-Q_t) vs t and t/Q_t vs t for pseudo first and second order kinetics and shown in Fig. 5b. The parameters calculated from Eqs. (1) and (2) are given in Table 2.

The Table 2 shows the comparison of the results and kinetic parameters of two kinetic models, Pseudo first model and Pseudo second- order model. The R^2 values showed that the data followed pseudo second kinetics and calculated value (Q_c) is closer to experimental value (Q_e) with greater correlation coefficient (R^2 = 0.9992). Therefore, it could be predicted that above data followed pseudo second order kinetics.

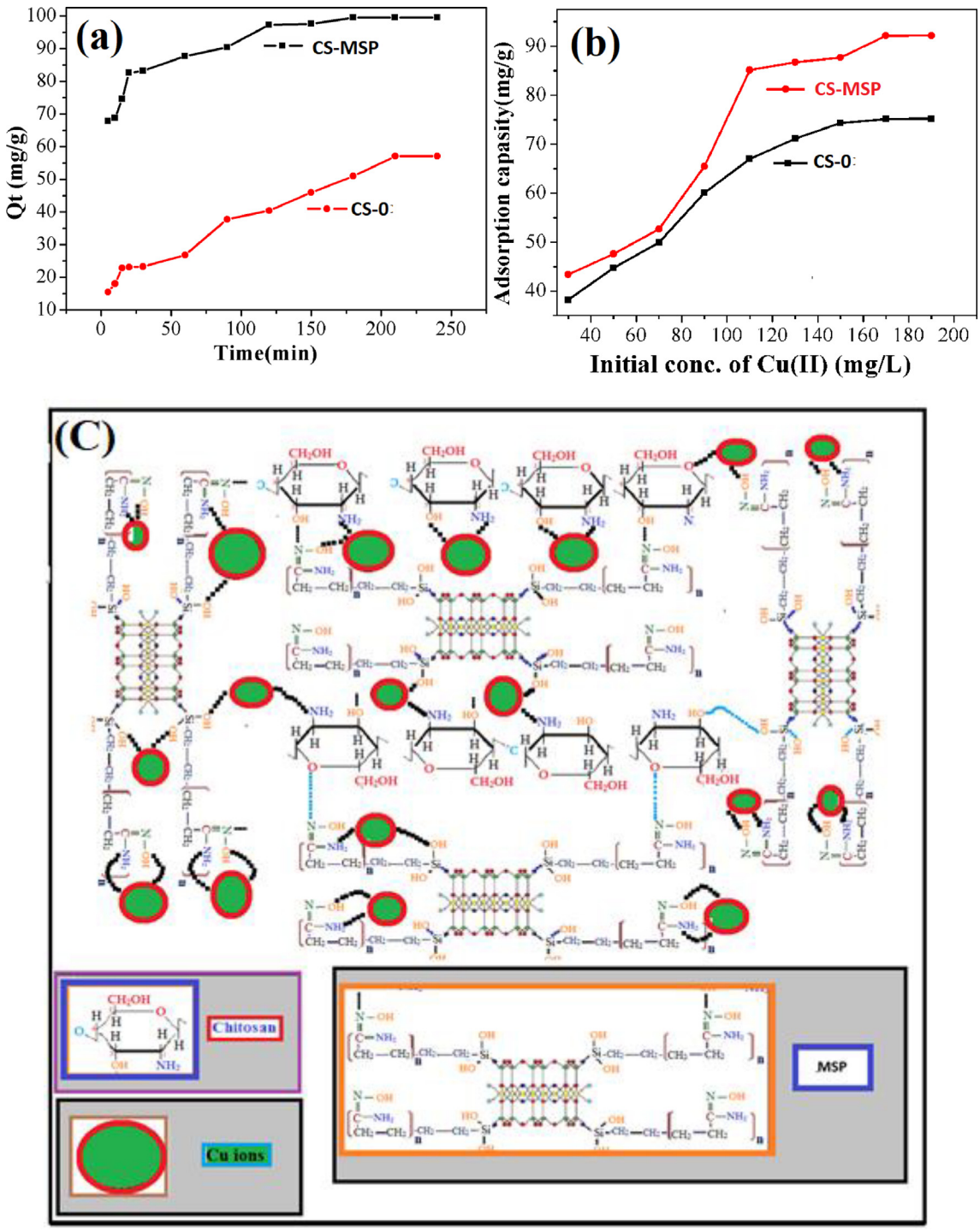

Fig. 4. Effect of contact time (a) and initial concentration (b) of Cu (II) on composite beads. (c) Proposed adsorption mechanism and scheme for Cu (II) uptake on CS-0 and CS-MSP beads.

3.4. Adsorption isotherms

Adsorption isotherm models demonstrate the interaction among the adsorbate concentration in solution and the amount of adsorbate adsorbed on the surface (mg g^{-1}). For the investigation of adsorption process, the Langmuir and Freundlich (El-Bahy and El-Bahy, 2016) isotherm models were applied to the experimental data.

Generally, the Langmuir model describes the adsorption process on definite homogeneous adsorbent sites inside the adsorbent. At constant temperature (T), the adsorption capacity is the function of the equilibrium concentration in solution. The Langmuir model assumes that: (i) on adsorbent surface, the adsorbed molecules form saturated mono-layer when adsorption occur, (ii) the enthalpy and energy of all adsorption sites are equal, and (iii) there are no interactions between adsorbed molecules after adsorption. Mathematically Langmuir isotherm can be expressed as:

$$\frac{C_e}{Q_e} = \frac{1}{K_L Q_m} + \frac{C_e}{Q_m} \tag{3}$$

Table 1
Surface area (BET), TGA analysis and Hydrolytic stability data of composite beads.

Sample	Surface area (m^2/g)	Pore Size (nm)	Pore volume (m^3/g)
CS-0	443.403	14.994	0.058
CS-MSP	435.887	15.058	0.015

Thermal Analysis			Hydrolytic stability		
Samples	Percentage residue (%)	T_{max} (°C)	Acidic medium (days)	Basic medium (days)	Aqueous medium (days)
CS-0	20.10	294.69	10	Up to several months	Up to several months
CS-MSP	32.05	298.71	30	Up to several months	Up to several months

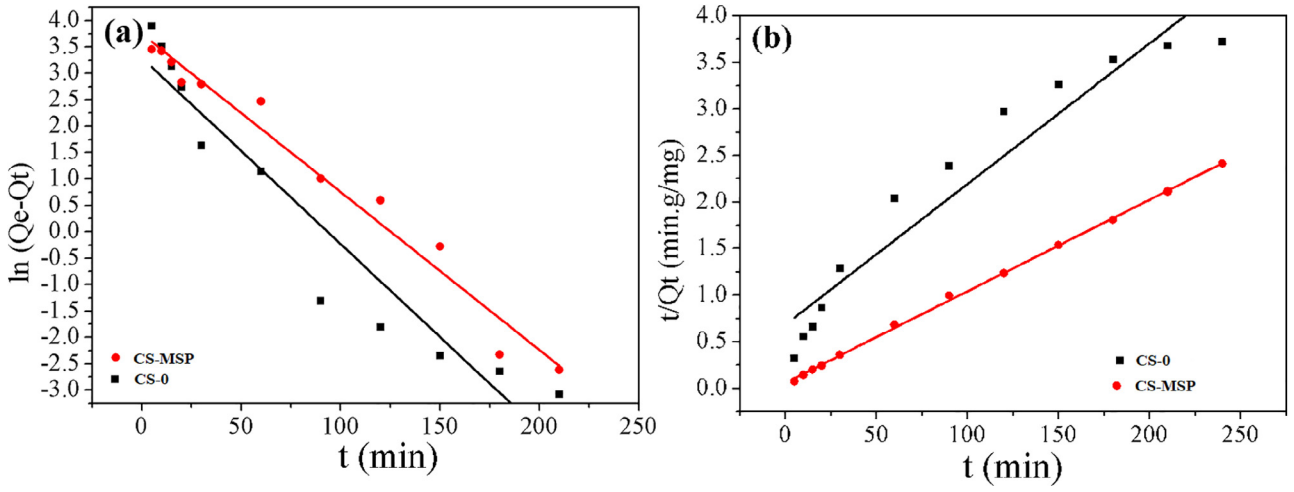

Fig. 5. Kinetic adsorption of Cu (II) (a) Pseudo-first-order and (b) Pseudo-second-order model for composite beads.

Table 2
Parameters of kinetic models for Cu (II) adsorption onto CS-0 and CS-MSP beads.

Pseudo First order Model Parameters				
Samples	Q_c (mg/g)*	K_1 (min^{-1})	Q_e (mg/g)!	R^2
CS-0	10.7810	−0.0077	65.075	0.9517
CS-MSP	10.4305	−0.0285	99.551	0.9105
Pseudo Second order Model				
Samples	Q_c (mg/g)*	K_2 (g mg^{-1} min^{-1})	Q_e (mg/g)!	R^2
CS-0	67.11	0.0031	65.075	0.9298
CS-MSP	102	0.0016	99.551	0.9992

Q_c*: Calculated value, Q_e!: Experimental value.

At equilibrium K_L (L/mg) is the Langmuir constant, C_e (mg L^{-1}) is the concentration of copper ion, and Q_m and Q_e are the adsorption capacities (mg g^{-1}). The graphical representation of Langmuir model is showed in Fig. 6a and Table 3 enlists the adsorption parameters.

The Freundlich adsorption isotherm model recommends the heterogeneity of the surface and assumes that adsorption occur on various energies sites. The adsorption energy varies as a function of surface coverage. Freundlich isotherm assumes that adsorption occur on heterogeneous surface on different energy sites and it forms a multi-layer. Freundlich adsorption isotherm is not fit for low concentrations and is fit for medium and high concentrations. Freundlich isotherm model is expressed as:

$$\ln Q_e = ln K_F + \frac{1}{n} \ln C_e \quad (4)$$

where n and K_F are the equilibrium adsorption constants for Freundlich isotherm. It is generally believed that if the n value is smaller than 1, then adsorption is not favorable while in the range of 2 to 10, adsorption is favorable (Daik et al., 2015). The Freundlich model is presented in Fig. 7b. The good fitting of the data suggests that the adsorption of copper ions on CS-0 and CS-MSP has mono-layer formation (Ijagbemi et al., 2009).

The Table 3 shows, equilibrium isotherm parameters values for the comparison of these two-isotherm model. The Langmuir model predicts higher Q_m* of 102 and 128 mg $g^{-1}$for CS-0 and CS-MSP, respectively. It was found that copper ions adsorption on (CS-0 and CS-MSP) followed Langmuir model more closely than Freundlich. Therefore, it could be concluded that the copper adsorption on both the adsorbents (CS-0 and CS-MSP) is homogeneous with a monolayer formation.

3.5. Methylene Blue removal

The adsorption performance of CS-0 and CS-MSP synthesized beads was investigated at different times for MB adsorption and depicted in Fig. 7. It was found that uptake of MB was progressively improved by increasing interaction time and eventually equilib-

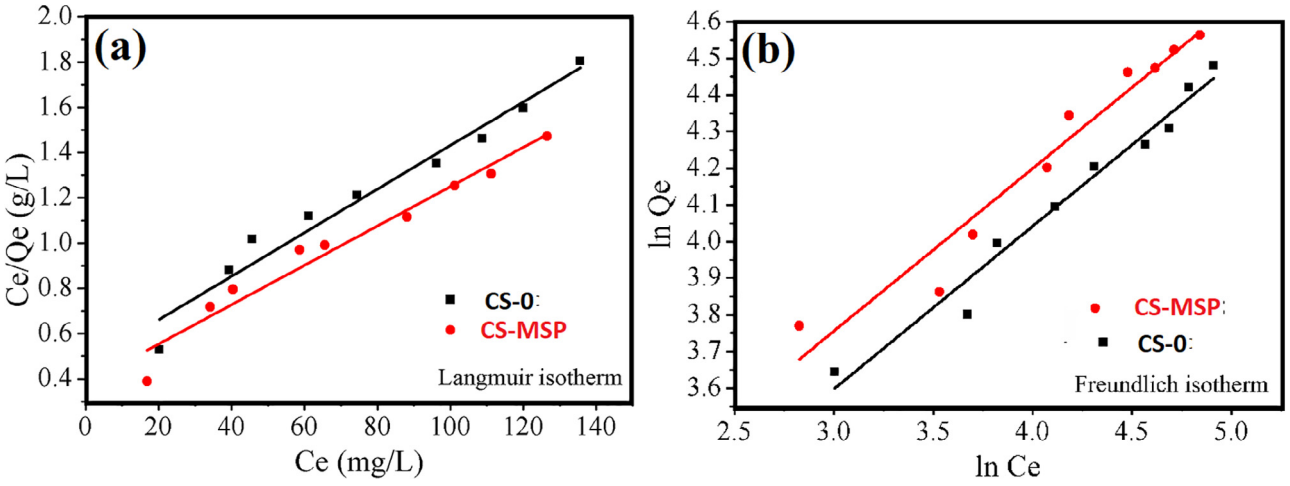

Fig. 6. Isotherm model fitting (a) Langmuir (b) Freundlich isotherm of Cu (II) uptake on composite beads.

Table 3
Equilibrium Isotherm constants for Cu (II) adsorption on composite beads.

Langmuir Isotherm Model				
Samples	Q_m*(mg/g)	K_L (L/mg)	Q_m! (mg/g)	R^2
CS-0	102	0.0226	75.17	0.9680
CS-MSP	128	0.0220	92.19	0.9830
Freundlich Isotherm				
Samples	n	K_f (mg/g) (L/mg) 1/n	R^2	
CS-0	2.424	6.3841	0.9377	
CS-MSP	2.880	6.6372	0.8979	

Q_m*: calculated value, Q_m!: Experimental value.

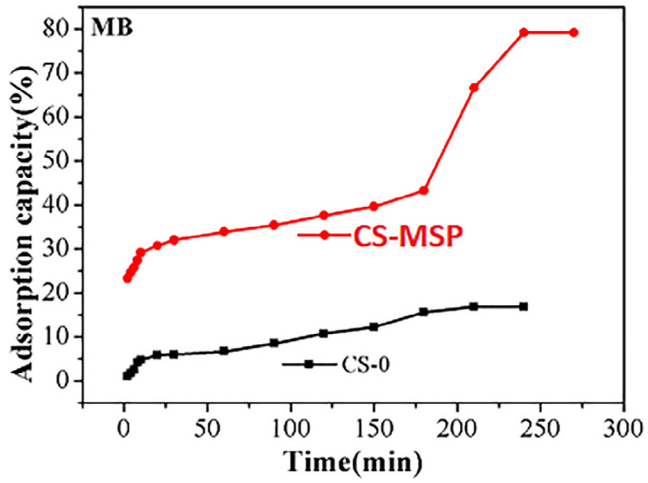

Fig. 7. Effect of contact time on adsorption of MB.

rium was achieved within 3.5 h. It can be seen from Fig. 7 that MB uptake by CS was expressively increased after MSP addition. The adsorption capacity of filler filled beads for MB was 80 mg/g.

4. Conclusions

This work demonstrates the development of organic–inorganic nanohybrid based bio-polymer composite system for the elimination of contaminants from wastewater. CS-amidoxime grafted sepiolite (MSP) composite beads (CS-MSP) were successfully fabricated. Addition of amidoxime grafted sepiolite as a filler into chitosan resulted in homogeneous dispersion for improving its physical, chemical, and adsorptive properties. CS-MSP composite beads were found mechanically and thermally stable. However, sepiolite addition decreased the surface area and pore volume of chitosan but surprisingly increased pore size. FT-IR results confirmed the interactions of sepiolite with chitosan matrix. The CS/MSP composite showed excellent adsorption capability for copper ions, with maximum adsorption of 99 mg/g for CS-MSP. Pseudo-second order kinetics was a better model for explaining the adsorption performance of copper ions. The adsorption data for both CS-0 and CS-MSP were best fitted with the Langmuir isotherm model. Maximum adsorption capacity (Q_m) was found to be 128 mg/g for CS-MSP and 102 mg/g for CS-0. The synthesized composite showed good adsorption towards MB as well. The current research suggested that nanohybrids based polymer composite beads can be synthesized by using easily available bio-materials and can be utilized as effective adsorbent for targeting various organic and inorganic pollutants present in wastewater.

Declaration of Competing Interest

The authors declare that they have no known competing financial interests or personal relationships that could have appeared to influence the work reported in this paper.

Acknowledgement

Researchers Supporting Project number (RSP-2021/348), King Saud University, Riyadh, Saudi Arabia.

References

Aksay, I.A., Kang, X., Liu, J., Lin, Y., Wang, C., Wang, D., Wu, H., Wang, J., 2009. Glucose biosensor based on immobilization of glucose oxidase in platinum nanoparticles/graphene/chitosan nanocomposite film. Talanta 80 (1), 403–406.

Alcântara, A.C., Aranda, P., Darder, M., Fernandes, F.M., Ruiz-Hitzky, E., Wicklein, 2013. Fibrous clays based bionanocomposites. Prog. Polym. Sci. 38 (10-11), 1392–1414.

Aldalbahi, A., El-Newehy, M.H., Moydeen, A.M., Thamer, B.M., 2020. In situ preparation of novel porous nanocomposite hydrogel as effective adsorbent for the removal of cationic dyes from polluted water. Polymers 12 (12), 3002.

Alhaddad, A., Durieu, C., Dantelle, G., Le Cam, E., Malvy, C., Treussart, F., Bertrand, J.-R., Tajmir-Riahi, H.-A., 2012. Influence of the internalization pathway on the efficacy of siRNA delivery by cationic fluorescent nanodiamonds in the Ewing sarcoma cell model. PloS One 7 (12), e52207.

Alhalaili, B., Matei, E., Predescu, A.M., Pantilimon, C., Tarcea, C., Vidu, R., 2020. Removal of heavy metals from wastewaters: a challenge from current treatment methods to nanotechnology applications. Toxics 8 (4), 101. https://doi.org/10.3390/toxics8040101.

Ali, N., Bilal, M., Khan, A., Nawaz, A., 2020. Fabrication and characterization of new ternary ferrites-chitosan nanocomposite for solar-light driven photocatalytic degradation of a model textile dye. Environ. Technol. Innov. 20, 101079. https://doi.org/10.1016/j.eti.2020.101079.

Alkan, M., Doğan, M., Demirbaş, Ö., Namli, H., Turan, P., Turhan, Y., 2008. Functionalized sepiolite for heavy metal ions adsorption. Desalination 230 (1-3), 248–268.

Arun, J., Bhatnagar, A., Bhargav, B.S., Gopinath, K.P., Srivatsav, P., Shanmugasundaram, V., 2020. Biochar as an Eco-Friendly and Economical Adsorbent for the Removal of Colorants (Dyes) from Aqueous Environment: A Review. Water 12 (12), 3561.

Atghia, S., Imanzadeh, G., Mansoori, Y., Sirousazar, M., Zamanloo, M., 2010. Polymer–clay nanocomposites: free-radical grafting of polyacrylamide onto organophilic montmorillonite. Eur. Polym. J. 46 (9), 1844–1853.

Ay, Ç.Ö., Özcan, A.S., Erdoğan, Y., Özcan, A., 2012. Characterization of Punica granatum L. peels and quantitatively determination of its biosorption behavior towards lead (II) ions and Acid Blue 40. Colloids Surf. B. Biointerfaces 100, 197–204.

Azeez, A.A., Rhee, K.Y., Park, S.J., Hui, D., 2013. Epoxy clay nanocomposites–processing, properties and applications: A review. Compos. Part B: Eng. 45 (1), 308–320.

Badawy, S.M., Dessouki, A.M., 2003. Cross-linked polyacrylonitrile prepared by radiation-induced polymerization technique. J. Phys. Chem. B 107 (41), 11273–11279.

Baek, M.-H., Ijagbemi, C.O., Kim, D.-S., 2009. Montmorillonite surface properties and sorption characteristics for heavy metal removal from aqueous solutions. J. Hazard. Mater. 166 (1), 538–546.

Bharti, V.S., Govindarajan, R.B., Kumar, K., Moorthy, A.K., Shukla, S.P., 2021. Acute toxicity of textile dye Methylene blue on growth and metabolism of selected freshwater microalgae. Environ. Toxicol. Pharmacol. 82, 103552.

Bhattacharya, A., Misra, B., 2004. Grafting: a versatile means to modify polymers: techniques, factors and applications. Prog. Polym. Sci. 29 (8), 767–814.

Bibi, S., Yasin, T., Hassan, S., Riaz, M., Nawaz, M., 2015. Chitosan/CNTs green nanocomposite membrane: Synthesis, swelling and polyaromatic hydrocarbons removal. Mater. Sci. Eng.: C 46, 359–365.

Bibi, S., Price, G.J., Yasin, T., Nawaz, M., 2016. Eco-friendly synthesis and catalytic application of chitosan/gold/carbon nanotube nanocomposite films. RSC Adv. 6 (65), 60180–60186.

Cuevas-Acuña, D.A.; Ezquerra-Brauer, J.M.; Plascencia-Jatomea, M.; Santacruz-Ortega, H.D.C.; Torres-Arreola, W.J., 2021. Development of Chitosan/Squid Skin Gelatin Hydrolysate Films: Structural, Physical, Antioxidant, and Antifungal Properties. *11* (9), 1088.

Daik, R., Jamil, S.N., Khairuddin, M., 2015. Preparation of acrylonitrile/acrylamide copolymer beads via a redox method and their adsorption properties after chemical modification. e-Polymers 15 (1), 45–54.

Duclaux, L., Kamal, M.A., Reinert, L., Yasin, T., 2016. Adsorptive removal of copper (II) ions from aqueous solution by silane cross-linked chitosan/PVA/TEOS beads: kinetics and isotherms. Desalin. Water Treat. 57 (9), 4037–4048.

El-Bahy, S.M., El-Bahy, Z.M., 2016. Synthesis and characterization of polyamidoxime chelating resin for adsorption of Cu (II), Mn (II) and Ni (II) by batch and column study. J. Environ. Chem. Eng. 4 (1), 276–286.

El-Sakhawy, M., Salama, A., Shukry, N., 2015. Carboxymethyl cellulose-g-poly (2-(dimethylamino) ethyl methacrylate) hydrogel as adsorbent for dye removal. Int. J. Biol. Macromol. 73, 72–75.

Feng, L., Li, X., Sarfaraz, K., Peng, Y., Zhao, C., Zhang, M., Zhang, Z., 2020. Novel cationic polymer modified magnetic chitosan beads for efficient adsorption of heavy metals and dyes over a wide pH range. Int. J. Biol. Macromol. 156, 289–301.

Galan, E., 1996. Properties and applications of palygorskite-sepiolite clays. Clay Miner. 31 (4), 443–453.

Gao, C., Ji, G., Wang, X., Wei, Y., Yuan, J., Zhu, G., 2017. Preparation of amidoxime functionalized SBA- 15 with platelet shape and adsorption property of U (VI). Separ. Purif. Technol. 174, 455–465.

García, N., Guzmán, J., Benito, E., Esteban-Cubillo, A., Aguilar, E., Santarén, J., Tiemblo, P., 2011. Surface modification of sepiolite in aqueous gels by using methoxysilanes and its impact on the nanofiber dispersion ability. Langmuir 27 (7), 3952–3959.

Ge, X., Xie, Y., Wang, J., Wang, M., 2015. Fabrication of fibrous amidoxime-functionalized mesoporous silica microsphere and its selectively adsorption property for Pb2+ in aqueous solution. J. Hazard. Mater. 297, 66–73.

Gull, N., Islam, A., Khan, S.M., Jamil, T., Munawar, M.A., Sabir, A., Shafiq, M., Yasin, T., 2016. Evaluation of selected properties of biocompatible chitosan/poly (vinyl alcohol) blends. Int. J. Biol. Macromol. 82, 551–556.

Hassan, M.I., Taimur, S., Yasin, T., 2017. Removal of copper using novel amidoxime based chelating nanohybrid adsorbent. Eur. Polym. J. 95, 93–104.

Ho, Y.-S., 2006. Review of second-order models for adsorption systems. J. Hazard. Mater. 136 (3), 681–689.

Kamal, M.A., Bibi, S., Bokhari, S.W., Siddique, A.H., Yasin, T., 2017. Synthesis and adsorptive characteristics of novel chitosan/graphene oxide nanocomposite for dye uptake. React. Funct. Polym. 110, 21–29.

Li, H., Huang, D., 2013. Microwave preparation and copper ions adsorption properties of crosslinked chitosan/ZSM molecular sieve composites. J. Appl. Polym. Sci. 129 (1), 86–93.

Malerba, M., Cerana, R., 2020. A review on chitin-and chitosan-based derivatives in plant protection against biotic and abiotic stresses and in recovery of contaminated soil and water. Polysaccharides 1 (1), 21–30.

Nasef, M.M., Güven, O., 2012. Radiation-grafted copolymers for separation and purification purposes: Status, challenges and future directions. Prog. Polym. Science. 37 (12), 1597–1656.

Parisi, F., 2020. Adsorption and separation of crystal violet, cerium (III) and lead (II) by means of a multi-step strategy based on K10-montmorillonite. Minerals 10 (5), 466.

Taimur, S., Yasin, T., 2017. Influence of the synthesis parameters on the properties of amidoxime grafted sepiolite nanocomposites. Appl. Surf. Sci. 422, 239–246.

Yuh-Shan, H., 2004. Citation review of Lagergren kinetic rate equation on adsorption reactions. Scientometrics 59 (1), 171–177.